



Meson resonances in forward-angle $\pi^+\pi^-$ photoproduction

Ł. Bibrzycki^{a,*}, P. Bydžovský^b, R. Kamiński^c, A.P. Szczepaniak^{d,e,f}

^a Institute of Computer Science, Pedagogical University of Cracow, 30-084 Kraków, Poland

^b Nuclear Physics Institute, CAS, 25068 Řež, Czech Republic

^c Institute of Nuclear Physics, Polish Academy of Sciences, Division of Theoretical Physics, 31-342 Kraków, Poland

^d Physics Department, Indiana University, Bloomington, IN 47405, USA

^e Center for Exploration of Energy and Matter, Indiana University, Bloomington, IN 47403, USA

^f Theory Center, Thomas Jefferson National Accelerator Facility, USA

ARTICLE INFO

Article history:

Received 20 September 2018

Received in revised form 4 December 2018

Accepted 19 December 2018

Available online 21 December 2018

Editor: V. Metag

Keywords:

Photoproduction

Partial wave analysis

Final state interactions

ABSTRACT

Assuming that the $\pi^+\pi^-$ photoproduction at forward angles and high energies is dominated by one pion exchange we calculate the $\pi^+\pi^-$ mass distributions for low partial waves. Predictions of the model agree well with the experimental data which indicate that the S , P and D waves are dominated by the $f_0(980)$, $\rho(770)$ and $f_2(1270)$, resonances respectively.

© 2018 The Authors. Published by Elsevier B.V. This is an open access article under the CC BY license (<http://creativecommons.org/licenses/by/4.0/>). Funded by SCOAP³.

Photoproduction is an important reaction in hadron spectroscopy. To determine resonance production mechanisms one performs partial wave analysis of the differential cross section in various final state channels. This is now possible thanks to availability of high-quality data from JLab, ELSA, MAMI, and SPring-8. Among those the CLAS data continues to be of high interest as it remains to be the only data on photoproduction of f_0 resonances. Specifically, from analysis of forward photoproduction of pseudoscalar mesons one can investigate the spectrum of light meson resonances, including those with exotic quantum numbers [1], which are important for development of our understanding of color confinement. In the previous studies we have shown that S and D resonances are copiously produced in di-pion photoproduction [2,3]. In those studies we assumed that the di-pion photoproduction is dominated by the t -channel ρ and ω exchanges at the nucleon vertex. In the present work we focus instead on the general properties of the production process. Specifically we examine two principal modes. The long-range mode related to the one pion exchange and the short-range one, which effectively takes into account all heavier meson exchanges and/or quark/gluon processes. As a function of the di-pion mass, the latter has singularities far away from the physical region and can be parametrized in terms

of a suitably chosen smooth functions. These two modes naturally arise when one considers restrictions imposed by unitarity on final state interactions in a general production process [4]. Instead of assuming a particular exchange mechanism, we generalize the conventional formulation of the Deck model [5,6] by applying the phenomenological set of pion-nucleon amplitudes obtained by the SAID group [7] and to describe the final state interactions in the $\pi\pi$ channel we use a set of partial wave amplitudes from a recent analysis in [8]. The use of phenomenological πN and $\pi\pi$ amplitudes enables us to make a prediction for the absolute normalization of the long range mode of the photoproduction amplitude, while the short range mode is fitted to the data. Resulting cross sections, as we show in this paper, agree well with the available data on the $\pi^+\pi^-$ photoproduction in the S , P , D , and F waves.

Model description. For the $\pi^+\pi^-$ photoproduction on the proton $\gamma(q, \lambda) + p(p_1, \lambda_1) \rightarrow p(p_2, \lambda_2) + \pi^+(k_1) + \pi^-(k_2)$, where λ 's denote particle helicities, the invariant amplitude is related to the S matrix by

$$S_{fi} = \delta_{fi} + i(2\pi)^4 \delta^4(p_2 + k_1 + k_2 - p_1 - q) \mathcal{T}_{fi}. \quad (1)$$

Accordingly, the invariant double-differential cross section expressed as a sum over $\pi\pi$ partial waves is given by

$$\frac{d^2\sigma}{d|t|d\sqrt{s}\pi\pi} = \frac{1}{64(2\pi)^4} \frac{|\mathbf{k}|}{(s-m^2)^2} \sum_{lm} \sum_{\lambda_2\lambda\lambda_1} |\mathcal{T}^{lm}|^2, \quad (2)$$

* Corresponding author.

E-mail address: lukasz.b@up.krakow.pl (Ł. Bibrzycki).

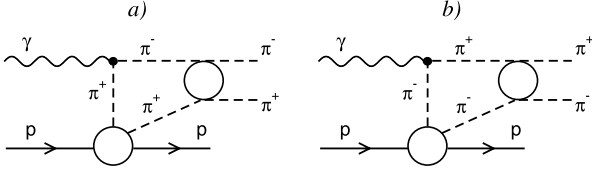


Fig. 1. Diagrams for the pion photoproduction (Deck mechanism), where pions are subject to final state interactions.

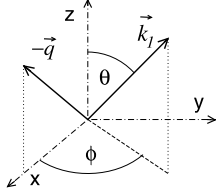


Fig. 2. Coordinate system in the $\pi\pi$ c.m. reference frame.

where $|\mathbf{k}| = \sqrt{s_{\pi\pi}/4 - m_\pi^2}$ is the magnitude of pion momenta in the $\pi\pi$ rest frame. The partial wave projection is defined in the $\pi\pi$ center of mass frame cf. Fig. 1. In this frame the direction of the recoil proton defines the negative z axis and y axis is perpendicular the di-pion production plane. The orientation of the π^+ momentum is given by the polar and azimuthal angles, θ and ϕ as shown in Fig. 2, with the photon momentum given by $\mathbf{q} = |\mathbf{q}|(-\sin\theta_q, 0, \cos\theta_q)$ where $|\mathbf{q}| = (s_{\pi\pi} - t)/2\sqrt{s_{\pi\pi}}$ and $\cos\theta_q$ is an algebraic function of the Mandelstam invariants.

In terms of the scattering amplitude \mathcal{T} the partial wave amplitudes are given by

$$\mathcal{T}^{lm} = \int d\Omega Y_{lm}^*(\Omega) \mathcal{T}(p_2\lambda_2 k_1 k_2, q\lambda p_1\lambda_1) \quad (3)$$

where $d\Omega = d\cos\theta d\phi$. The partial wave amplitudes depend on the total invariant energy $s = (q + p_1)^2$, momentum transfer $t = (p_2 - p_1)^2$, and $\pi\pi$ invariant mass $\sqrt{s_{\pi\pi}}$. A similar expression holds for the Deck amplitude \mathcal{M}^{lm} (see below).

For each spin, l and isospin, $I = 0, 1, 2$ the final state interactions are described by the $\pi\pi$ partial wave amplitudes, t_l^I that are given by the phase shifts δ_l^I and inelasticity parameters η_l^I ,

$$t_l^I = \frac{1}{2i\rho} \left(\eta_l^I e^{2i\delta_l^I} - 1 \right), \quad (4)$$

where $\rho = 2|\mathbf{k}|/\sqrt{s_{\pi\pi}}$. The partial wave amplitudes $t_l^I(s_{\pi\pi})$ are taken from the recent study of [8], where crossing symmetry and once subtracted dispersion relations were imposed to further constrain the amplitudes that were studied previously in [9–11].

In the limit of a large production range, the partial waves are related to the FSI amplitudes by a simple algebraic relation [4], which for the even waves, assuming isospin symmetry reads,

$$\begin{aligned} \mathcal{T}_{\pi^+\pi^-(\lambda_2\lambda\lambda_1)}^{lm} \\ = \left[1 + i\rho \left(\frac{2}{3}t_l^0 + \frac{1}{3}t_l^2 \right) \right] \mathcal{M}_{\pi^+\pi^-(\lambda_2\lambda\lambda_1)}^{lm}, \end{aligned} \quad (5)$$

and for the odd ones

$$\mathcal{T}_{\pi^+\pi^-(\lambda_2\lambda\lambda_1)}^{lm} = [1 + i\rho t_l^1] \mathcal{M}_{\pi^+\pi^-(\lambda_2\lambda\lambda_1)}^{lm}. \quad (6)$$

Here the long-range production, \mathcal{M}^{lm} is taken as the partial wave projection of one pion exchange aka the Deck amplitude. The Deck amplitude was originally constructed in [5] under the assumption that contribution from the nearest singularity at low- $t_{\gamma\pi}$, which is the channel dual to $s_{\pi\pi}$, is that of the pion pole. Moreover, gauge

invariance was imposed by modifying the pion pole according to a following prescription [6],

$$\begin{aligned} M_{\lambda_2\lambda\lambda_1} = -e \left[\left(\frac{\epsilon_\lambda \cdot k_2}{q \cdot k_2} - \frac{\epsilon_\lambda \cdot (p_1 + p_2)}{q \cdot (p_1 + p_2)} \right) T_{\lambda_1\lambda_2}^+ \right. \\ \left. - \left(\frac{\epsilon_\lambda \cdot k_1}{q \cdot k_1} - \frac{\epsilon_\lambda \cdot (p_1 + p_2)}{q \cdot (p_1 + p_2)} \right) T_{\lambda_1\lambda_2}^- \right] \end{aligned} \quad (7)$$

where e is the electric charge, ϵ_λ is the photon helicity polarization vector and $T_{\lambda_1\lambda_2}^+$ and $T_{\lambda_1\lambda_2}^-$ are $\pi^\pm N$ scattering amplitudes. This is one of many possible implementations of gauge invariance. Another model, for example, was studied in [12] where contributions from the baryon exchanges were also included, which required a different modification to make the overall amplitude gauge invariant. In the following we use Eq. (7), which appears better suited in the kinematics dominated by meson exchanges. Similarly to \mathcal{T}^{lm} the partial wave projection of the Deck amplitude is given by,

$$\mathcal{M}_{\pi^+\pi^-(\lambda_2\lambda\lambda_1)}^{lm} = \int d\Omega Y_{lm}^*(\Omega) M_{\lambda_2\lambda\lambda_1}. \quad (8)$$

Elastic amplitudes of the π^+ and π^- scattering off protons that appear in Eq. (7) can be expressed in terms of the isospin amplitudes

$$T_{\lambda_1\lambda_2}^+ = T_{\lambda_1\lambda_2}^{\frac{3}{2}}, \quad T_{\lambda_1\lambda_2}^- = \frac{1}{3}(T_{\lambda_1\lambda_2}^{\frac{3}{2}} + 2T_{\lambda_1\lambda_2}^{\frac{1}{2}}), \quad (9)$$

with the latter given in terms of the standard Lorentz invariant isospin amplitudes [13]

$$T_{\lambda_1\lambda_2}^I = \bar{u}(p_2, \lambda_2) (A^I + \gamma \cdot Q B^I) u(p_1, \lambda_1) \quad (10)$$

with $Q = \frac{1}{2}(q \mp k_1 \pm k_2)$, for π^- and π^+ scattering, respectively. To construct the amplitudes in Eq. (9) we use the SAID πN partial wave parametrization. Note that due to kinematics of the process the pion that undergoes the scattering on the proton target is not on its mass shell: $(q - k_1)^2 \neq m_\pi^2$. Consistency with the assumed one pion exchange nature of the leading singularity demands, however, that the πN amplitudes are evaluated on-shell and that the pion virtuality only appears through the pion propagator (cf. Fig. 1). Even though the pion exchange is close to the physical region, because of the finite momentum transfer between the target and recoil nucleon, t the Deck amplitude gives a rather smooth function of $s_{\pi\pi}$. In Fig. 3 we compare individual cross sections computed for each of the four lowest partial waves (S, P, D, F) of the Deck amplitude, with their incoherent sum in Eq. (2) and with

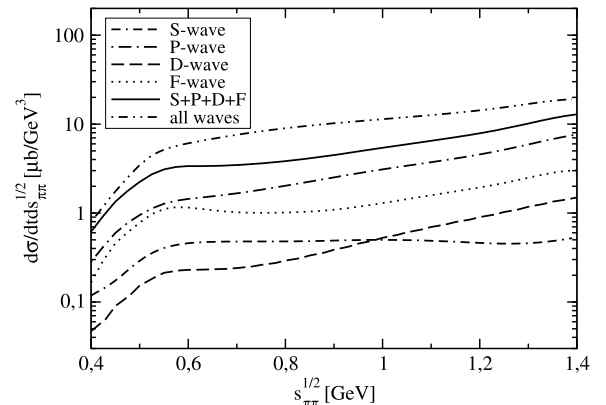


Fig. 3. Cross sections for low partial waves as compared to the cross section computed from the complete amplitude. The results are calculated without the final state interactions.

the total, unprojected Deck amplitude (“all waves”). The calculation is done at photon energy $E_\gamma = 3.3$ GeV and momentum transfer squared $t = -0.55$ GeV². We observe that the convergence rate of the partial wave expansion is rather slow, so that the combined four lowest waves account for roughly 50% of the total contribution to the $s_{\pi\pi}$ intensity distribution. Moreover, the clear hierarchy of partial waves is visible, with the odd partial waves being stronger than the even ones. This can be understood by considering the $\cos\theta$ and ϕ dependence of $T_{\lambda_1\lambda_2}^+$ and $T_{\lambda_1\lambda_2}^-$ in Eq. (7). Changing $\theta \rightarrow \pi - \theta$ and $\phi \rightarrow \phi + \pi$ in the second term of Eq. (7) and using Eq. (9) we see that the partial wave expansion in Eq. (8) can be rewritten as

$$\mathcal{M}_{\pi^+\pi^-}^{lm} = -e \int d\Omega Y_{lm}^*(\Omega) \left(\frac{\epsilon_\lambda \cdot k_2}{q \cdot k_2} - \frac{\epsilon_\lambda \cdot (p_1 + p_2)}{q \cdot (p_1 + p_2)} \right) \times \left[T^{\frac{3}{2}} - \frac{(-1)^l}{3} (T^{\frac{3}{2}} + 2T^{\frac{1}{2}}) \right]. \quad (11)$$

It thus follows that in the case of even partial waves, $l = 0, 2, \dots$, the dominant πN isospin 3/2 component is partially canceled while in odd ones it is enhanced, which explains qualitatively the hierarchy observed in Fig. 3.

Numerical results. In general, in the kinematics discussed here, a minimal model for $\pi^+\pi^-$ photoproduction should contain two parts. One corresponds to production of pion pairs from a spatially extended region and is given by Eqs. (5) and (6). We refer to this component as “Deck+FSI”. The other, corresponds to production from a spatially compact source. For each partial wave the latter can be parametrized by a short-range contribution given by,

$$(A + B s_{\pi\pi}) e^{i\delta_l^I} \sin\delta_l^I \quad (12)$$

The term in the parentheses effectively parametrizes the smooth $s_{\pi\pi}$ dependence, which in the physical region arises from exchanges of heavier mesons and/or quarks. This term is modified in the standard way by final state interactions in the $\pi\pi$ channel, where, given the limited data range, we ignore inelastic effects. The free parameters A and B were fitted to experimental mass distributions extracted from the CLAS data. We compare predictions of the model with the mass distributions for low partial waves determined by the CLAS collaboration [14], which, to our knowledge, are the only available data on the di-pion partial-wave mass distributions.

In Fig. 4 we compare model predictions with the experimental S -wave mass distribution which we denote here by CLAS fit as it was obtained from fitting the measured data [14]. It is clear that already the Deck amplitude alone gives the right magnitude of mass distribution and reproduces the mass dependence of background, i.e. outside the region of the $f_0(980)$ resonance. When the final state $\pi\pi$ interactions are taken into account (“Deck+FSI”), the resonant shape around 1 GeV, is well reproduced. Destructive interference between direct di-pion production and final state interaction *cf.* Eq. (5) results in the mass distribution dipping below the experimental points in the whole energy region (see the discussion below Fig. 6 for more details). If, however, we include the short range component with parameters $A = -14.5 \pm 0.6$ GeV⁻¹ and $B = 2.7 \pm 0.6$ GeV⁻³ the fit fairly reproduces the mass distribution behavior both in resonance region and outside. The slightly different invariant mass behavior of our predictions above 1 GeV in comparison with the CLAS fit can be attributed to the absence of the $K\bar{K}$ channel in the model. Another point we would like to discuss here is a contribution of the correction term in Deck amplitude, Eq. (7) required for gauge invariance, typically referred to as a contact term (even though in our case it is not local). In Fig. 4

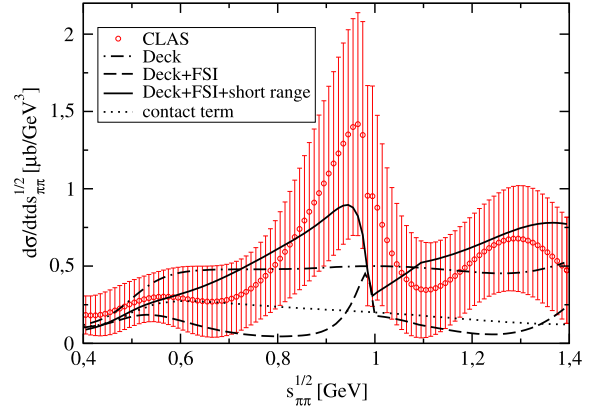


Fig. 4. S -wave double differential cross section at $E_\gamma = 3.3$ GeV and $-t = 0.55$ GeV². Dash-dotted line – pure Deck model; dashed line – Deck model with final state $\pi\pi$ interactions; solid line – Deck model with FSI and the short range term; dotted line – contribution of the contact term; red points – CLAS fit to the experimental data. The error band shows the total uncertainty that combines the systematic and statistical uncertainties.

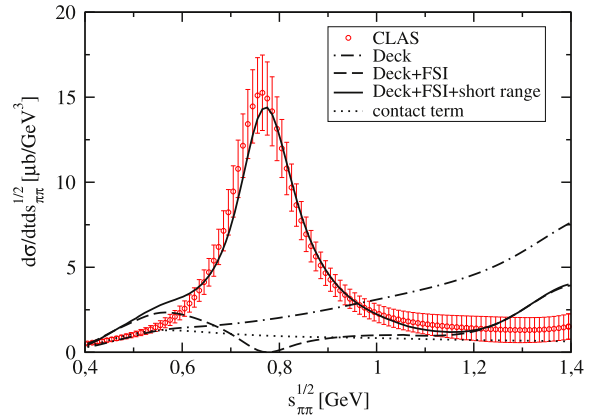


Fig. 5. P -wave double differential cross section at $E_\gamma = 3.3$ GeV and $-t = 0.55$ GeV². Dash-dotted line – pure Deck model; dashed line – Deck model with final state $\pi\pi$ interactions; solid line – Deck model with FSI and the short range term; dotted line – contribution of the contact term; red points – CLAS fit to the experimental data. The band shows the total uncertainty of the fit.

we show the contribution of the contact term in Eq. (7) (the dotted line). It is apparent that in the region around 0.6 GeV this contribution reveals a small enhancement in the mass distribution. This enhancement is also seen in the curve obtained from the “Deck+FSI” amplitude. One can also say that the contribution is relatively large in the S wave.

In Fig. 5 we show the CLAS P -wave mass distribution compared to our model predictions. The overall agreement of data with the full model (Deck+FSI+short range), especially in the resonance region, is good. However, the long-range component with final state interactions (Deck+FSI) produces a minimum rather than the maximum at the resonance energy. Thus the peak of the $\rho(770)$ resonance, as expected is due to the short range production. Specifically we find $A = 48.9 \pm 1.6$ GeV⁻¹ and $B = -24.3 \pm 2.0$ GeV⁻³. A comparison of the fitted values of the A and B parameters for the S and P waves implies that the relative contribution of the short range component of the amplitude is much larger in the P wave, as expected for the standard $q\bar{q}$ state. Small deviations from the data can be observed in the near threshold region and for masses well above the $\rho(770)$ mass. The near threshold discrepancy results from a small enhancement in the contact term magnified by final state interactions. An alternative model for the P -wave

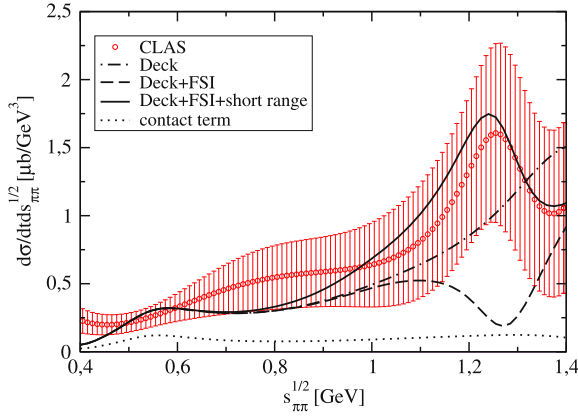


Fig. 6. D -wave double differential cross section at $E_\gamma = 3.3$ GeV and $-t = 0.55$ GeV² with $M \leq 1$. Dash-dotted line – pure Deck model; dashed line – Deck model with final state $\pi\pi$ interactions; solid line – Deck model with FSI and the short range term; dotted line – contribution of the contact term; red points – CLAS fit to the experimental data. The band shows the total uncertainty of the fit.

photoproduction of $K\bar{K}$, based on the pomeron exchange dominance, can be found in [15], which also applies to the $\pi^+\pi^-$ case.

In Fig. 6 we show our model results compared to CLAS D -wave mass distribution. It is important to note that following the experimental analysis we take into account only the amplitudes where the magnetic quantum number M of the $\pi\pi$ system (equivalent to the helicity in the chosen frame of reference) is smaller than 2. Similarly as in the S wave, the model gives the right magnitude of the experimental points even for the pure Deck amplitude. Recall that this result is parameter free, contrary to the results in Ref. [3] that were fitted to the experiment. Inclusion of the final state interactions, similarly as in the P -wave, results in developing the minimum rather than the maximum for the invariant masses around the $f_2(1270)$. This different pattern in the S and D waves can be understood from behavior of the isoscalar $\pi\pi$ phase shifts [8]. The production amplitude in Eq. (5) is dominated by the term proportional to $\cos\delta_1^0$, which comes from the square brackets in Eq. (5). Then the minimum in the D wave is due to the $\pi\pi$ phase shift passing $\pi/2$ at about 1.25 GeV. In the S wave the phase first passes $\pi/2$ at about 0.85 GeV as seen in Fig. 4 for “Deck+FSI”. When the S wave phase shift reaches π at $\sqrt{s_{\pi\pi}} \sim 0.95$ GeV it produces a maximum. The model agrees much better with the D -wave data if we include the short range component with parameters $A = -24 \pm 11$ GeV⁻¹ and $B = 10 \pm 7$ GeV⁻³. It is obvious from Eq. (12) that the D wave resonates at $\sqrt{s_{\pi\pi}} \sim 1.25$ GeV (so, the overall amplitude behavior is quite analogous as in the P -wave). The contribution of the contact term is not so important in the D wave as in the S wave but it also reveals a tiny bump below 0.6 GeV that is apparent in the full result (the solid line).

In Fig. 7 we compare the model prediction with the F -wave mass distribution measured by CLAS. A discrepancy is observed throughout the entire mass region. Moreover, the effect of the final state interactions in the F wave is negligible, which results from very small values of $\pi\pi$ partial waves. On the other hand the effect of the contact term is relatively large here and it explains the bump around 0.6 GeV. It is apparent that a form of the contact term is responsible for the excess in the mass distribution below 0.8 GeV, as indicated by the double-dash-dotted line. As the contribution of the contact term is flat it cannot contribute to the rising distribution at high masses.

Conclusions and outlook. With the model discussed in this paper we have calculated mass distributions for various partial waves in photoproduction of the $\pi^+\pi^-$ pairs on the proton. In our

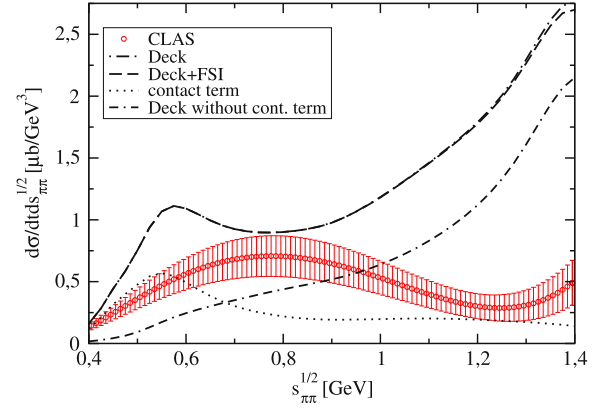


Fig. 7. F -wave double differential cross section at $E_\gamma = 3.3$ GeV and $-t = 0.55$ GeV² and $M \leq 1$. Dash-dotted line – pure Deck model; dashed line – Deck model with final state $\pi\pi$ interactions; dotted line – contribution of the contact term; double-dash-dotted line – Deck without the contact term; red points – CLAS fit to the experimental data. The band shows the total uncertainty of the fit.

approach we combine the Deck model, which accounts for the extended source mode of the photoproduction, with the SAID parametrization of πN scattering amplitudes. This part of the model is essentially parameter free. Thus, we have probed the dominant exchange mechanism of the reaction at forward angles that is given by the one pion exchange in the $t_{\gamma\pi}$ channel. We also took into account the compact source mode of the reaction, which based on the general grounds can be parametrized by a smooth function. In this respect we have used a first order polynomial in $s_{\pi\pi}$. When we include the final state $\pi\pi$ interactions in the model, we obtain the $\pi\pi$ mass distributions which for low partial waves are in good agreement with CLAS measurements made at $E_\gamma = 3.3$ GeV. Predictions of the model agree well with the experimental fact that the S and D waves are dominated by isoscalar $f_0(980)$ and $f_2(1270)$ resonances, respectively, whereas the P wave is dominated by the isovector $\rho(770)$ resonance. Moreover, we observe that the compact source component of the resonant amplitude in P and D waves is larger than this same component for the S wave (compare e.g. the values of the corresponding A and B parameters). This is in line with the expectation that while the $\rho(770)$ and $f_2(1270)$ are typical $q\bar{q}$ resonances, the $f_0(980)$ is rather more loosely bound system of four quarks. In the F wave we observed the discrepancy between CLAS measurements and model predictions. At small invariant masses we attribute this discrepancy to a specific form of the contact term adopted from [6]. We observe a general hierarchy of the partial waves resulting from the pure Deck model, namely that the even partial waves are weaker than the odd ones which can be qualitatively inferred from Eq. (11).

A similar analysis using the Deck (Drell) mechanism driven by the kaon exchange for the $K\bar{K}$ photoproduction was performed in [16]. In their analysis the authors took into account the full KN and $\bar{K}N$ scattering amplitudes showing that the kaon exchange mechanism alone is not sufficient to describe the data on the K^+p and K^-p invariant mass spectra. The reaction mechanism was therefore extended by adding the K^* exchange with a large coupling to the $\Lambda(1520)$ resonance and a better description of the invariant mass spectra was achieved. Our findings are consistent in that the reaction mechanism based only on the long range mode is not enough to get a realistic description of the data. The two-pion photoproduction on the nucleon was also studied at small energies ($E_\gamma < 1.5$ GeV) in [17] based on an effective Lagrangian approach. To achieve a satisfactory description of the data on total cross sections the authors included many baryon resonances in

the s -channel with the mass below 1.8 GeV. In the t -channel, exchanges of heavier mesons (σ and ρ) were included showing that also in this approach far-away singularities do play important role.

Our formalism allows for systematic refinements of the model. These include the coupled channel effects (which we expect to be important especially for the isoscalar S wave), off-shell effects and inclusion of other t -channel exchanges. In order to use the model in the full kinematic region accessible for GlueX and CLAS12 energies, the SAID πp amplitudes must be supplemented with amplitudes applicable for πp CM energies beyond 2 GeV.

Acknowledgements

Authors acknowledge fruitful discussions with members of the JPAC collaboration. This work was supported by the Grant Agency of the Czech Republic under the grant No. P203/15/04301, the U.S. Department of Energy under grants No. DE-AC05-06OR23177 and No. DE-FG02-87ER40365, and the U.S. National Science Foundation under award numbers PHY-1507572, PHY-1415459 and PHY-1205019. This work has also been partially supported by the Polish Science Center (NCN) Grant No. 2018/29/B/ST2/02576.

References

- [1] A.P. Szczepaniak, M. Swat, Phys. Lett. B 516 (2001) 72.
- [2] Chueng-Ryong Ji, R. Kamiński, L. Leśniak, A. Szczepaniak, R. Williams, Phys. Rev. D 58 (1998) 1205.
- [3] Ł. Bibrzycki, R. Kamiński, Phys. Rev. D 87 (2013) 114010.
- [4] I.J. Aitchison, M.G. Bowler, J. Phys. G 3 (1977) 1503.
- [5] R.T. Deck, Phys. Rev. Lett. 13 (1964) 169.
- [6] J. Pumplin, Phys. Rev. D 2 (1970) 1859.
- [7] SAID, R.L. Workman, R.A. Arndt, W.J. Briscoe, M.W. Paris, I.I. Strakovsky, Phys. Rev. C 86 (2012) 035202, <http://gwdac.phys.gwu.edu/>.
- [8] P. Bydžovský, R. Kamiński, V. Nazari, Phys. Rev. D 94 (2016) 116013.
- [9] P. Bydžovský, R. Kamiński, V. Nazari, Phys. Rev. D 90 (2014) 116005.
- [10] Yu.S. Surovtsev, P. Bydžovský, R. Kamiński, M. Nagy, Phys. Rev. D 81 (2010) 016001.
- [11] R. Garcia-Martin, R. Kaminski, J.R. Pelaez, J. Ruiz de Elvira, F.J. Yndurain, Phys. Rev. D 83 (2011) 074004.
- [12] P. Stichel, M. Scholz, Nuovo Cimento 34 (1964) 1381.
- [13] G. Chew, M. Goldberger, F. Low, Y. Nambu, Phys. Rev. 106 (1957) 1337.
- [14] M. Battaglieri, et al., CLAS collaboration, Phys. Rev. D 80 (2009) 072005.
- [15] L. Leśniak, A.P. Szczepaniak, Acta Phys. Pol. B 34 (2003) 3389.
- [16] A. Sibirtsev, J. Haidenbauer, S. Krewald, U.-G. Meissner, A.W. Thoms, Eur. Phys. J. A 31 (2007) 221.
- [17] A. Fix, H. Arenhövel, Eur. Phys. J. A 25 (2005) 115.